Accepted Manuscript

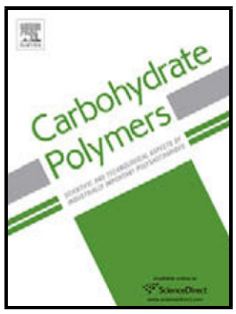

Title: Physicochemical and structural properties of pregelatinized starch prepared by improved extrusion cooking technology

Authors: Yunfei Liu, Jun Chen, Shunjing Luo, Cheng Li, Jiangping Ye, Chengmei Liu, Robert G. Gilbert

PII: S0144-8617(17)30860-3
DOI: http://dx.doi.org/doi:10.1016/j.carbpol.2017.07.084
Reference: CARP 12601

To appear in:

Received date: 10-3-2017
Revised date: 24-7-2017
Accepted date: 29-7-2017

Please cite this article as: Liu, Yunfei., Chen, Jun., Luo, Shunjing., Li, Cheng., Ye, Jiangping., Liu, Chengmei., & Gilbert, Robert G., Physicochemical and structural properties of pregelatinized starch prepared by improved extrusion cooking technology.*Carbohydrate Polymers* http://dx.doi.org/10.1016/j.carbpol.2017.07.084

Physicochemical and structural properties of pregelatinized starch prepared by improved extrusion cooking technology

Yunfei Liu [a], Jun Chen [a], Shunjing Luo [a], Cheng Li [c], Jiangping Ye [a], Chengmei Liu [a,*], Robert G. Gilbert [b, c]

[a] State Key Laboratory of Food Science and Technology, Nanchang University, Nanchang 330047, China

[b] Centre for Nutrition and Food Sciences, Queensland Alliance for Agriculture and Food Innovation, The University of Queensland, Brisbane, QLD, Australia

[c] Joint International Research Laboratory of Agriculture and Agri-Product Safety, College of Agriculture, Yangzhou University, Yangzhou Jiangsu Province 225009, China

*Corresponding author: Chengmei Liu

Address: State Key Laboratory of Food Science and Technology, Nanchang University, Nanchang 330047, China.

Tel. /Fax: +86-791-88305871

E-mail address: liuchengmei@aliyun.com

Highlights:

- Pregelatinized starch (IPS) was prepared by Improved Extrusion Cooking Technology.
- IPS had improved solubility, gel stability & lower short-term retrogradation rate.
- The chains near or at the branching points were degraded during IECT process.
- Functional properties were explained in terms of changes in starch structure.

Abstract

Pregelatinized starch was made from indica rice starch using a so-called "improved extrusion cooking technology" (IECT) under 30%-70% moisture content. IECT-pregelatinized starch (IPS) had higher water solubility and water absorbability compared to native starch at low temperature. For pasting properties, the breakdown and setback viscosities of IPS were significantly ($p < 0.05$) lower than native starch, suggesting improved gel stability and reduced short-term retrogradation. The rice starch granules lost their integrity in IPS, and formed a honeycomb-like structure with increased moisture content in the raw material. These properties can be explained in terms of molecular structural features, particularly the large reduction in the size of molecules, but without significant changes in the chain-length distributions of amylopectin component, and no significant change in amylose fraction. These results indicate that IECT is suitable for preparing IPS with desirable water solubility and gel stability properties.

Keywords: Pregelatinized starch; indica rice starch; improved extrusion cooking

technology; structure; physicochemical properties

1. Introduction

Starches are biodegradable and relatively inexpensive natural biopolymers which are widely used in food and pharmaceutical industries (Hoover, Hughes, Chung, & Liu, 2010). However, native starches have some limitations such as low water solubility and undesirable retrogradation after gelatinization under some circumstances (Fu, Wang, Li, & Adhikari, 2012). In order to overcome such drawbacks, physical, chemical, and/or enzymatic modifications of starch are necessary (Din, Xiong, & Fei, 2015).

Pregelatinized starch is a kind of physically modified starch with cold-water-swelling capacity and desirable pasting and texturizing properties (Miyazaki, Van Hung, Maeda, & Morita, 2006). It is of great use in production of sustained release tablets with good cold-water-swelling capacity and gel barrier formation properties (Sánchez, Torrado, & Lastres, 1995). Fu, Che, Li, Wang, and Adhikari (2016) reported that the rheological properties of dough made from the pregelatinized starch in the granular state had increased storage (G′) and loss (G″) moduli but decreased sensitivity to the frequency compared to the parent starch. Cold-water-swelling capacity and low gelatinized temperature make pregelatinized starch desirable.

Pregelatinized starch can be produced through many physical processes such as spray drying (Laovachirasuwan, Peerapattana, Srijesdaruk, Chitropas, & Otsuka,

2010), drum drying (Hedayati, Shahidi, Koocheki, Farahnaky, & Majzoobi, 2016), high hydrostatic pressure (Li et al., 2011), thermomechanical processing (Barron, Buleon, Colonna, & Della, 2000) and extrusion cooking (Sánchez, Torrado, & Lastres, 1995; Della, Vergnes, Colonna, & Patria, 1997) followed by drying. Among these technologies, extrusion cooking is recommended as being a shorter and more flexible process when compared to other processes, and has been widely applied to the production of cereal-based snack-like products (Sacchetti, Pinnavaia, Guidolin, & Rosa, 2004). Conventional extrusion cooking is a continuous high-temperature and short-time process, which physically modifies moistened expansible starchy and proteinaceous material, and makes the material swell through the unique combination of high temperature, pressure and shear forces (Camire, Camire, & Krumhar, 1990).

What we term “Improved Extrusion Cooking Technology” (IECT) is a new gelatinization technology, which is significantly different from traditional single-screw extruders. Our transformed single-screw extruder shows the characteristics of a longer screw (1950 cm), longer residence time (18–90 s), lower temperature (50–150 ^{o}C) and lower screw speed (15–75 rpm) than traditional extrusion cooking extruders; these differences make the material expand to change the extrudate structure so as to improve extrudate properties (Liu et al., 2011). In our previous work, texturized rice prepared by IECT was rich in nutrients and showed similar texture properties and shape to polished rice (Liu et al., 2011). Further, modified high-amylose rice starch prepared by IECT had a lower percentage of retrogradation and a lower retrogradation rate (Zhang et al., 2014). This technology

also improved the freeze-thaw stability of starch (Ye et al., 2016). These results suggest that IECT has the potential to modify physical and chemical properties of starch to give some desirable functional properties. However, there has been little research on the molecular mechanism underlying the changes caused by the process.

In this study we report the preparation of pregelatinized rice starch by IECT and characterize its water solubility and absorption, pasting properties, and the changes in the crystalline and molecular structure brought about by the process. The relationship between physicochemical and structural properties of IECT-pregelatinized starch (IPS) was investigated, and the underlying molecular mechanism discussed.

2. Materials and methods

2.1 Materials

Rice starch was obtained from Golden Agriculture Biotech Co., Ltd. (Jiangxi, China). It had a moisture content of 6% (w/w, wet basis) (AOAC, 2005), amylose content of 22% as calculated from the size-exclusion chromatography (SEC) data (see SEC analysis), 2% fat and 0.34% protein. Pullulan standards (peak molecular weights: 342-2.35 × 10^6 Da) with known peak molecular weights were purchased from Polymer Standards Service (PSS, Mainz, Germany). Dimethyl sulfoxide (DMSO, GR grade for analysis) was purchased from Merck Co. Inc. (Australia). All other chemicals were of reagent grade and used as received.

2.2 Preparation of IPS by IECT

The IECT treatment was executed as previously described (Ye et al., 2016), and performed on a single-screw extruder (designed by our laboratory, and produced in Jinan Saixin Machinery Ltd., China) with a screw length of 1950 mm and diameter of 100 mm (Liu et al., 2011). The moisture contents (wet basis) of raw material for each sample were adjusted to 30%, 40%, 50%, 60%, and 70% by adding water followed by intense stirring using an agitator before IECT processing. The independent processing variables for the extrusion were as follows: screw feed rate was 30 kg/h, screw speed was 37.5 rpm. In addition, the temperature profiles in the feed, mix, screw conveyor, shearing compression metering, die zones were kept constant at 50, 65, 85, 100 and 95°C. The temperatures were chosen following our previous research on the preparation of texturized rice which showed similar texture properties to polished rice, but also contained comprehensive nutrients (Liu et al., 2011). We found that over this temperature range, the rice starch had a lower retrogradation rate and improved freeze-thaw stability after IECT processing (Ye et al., 2016; Zhang et al., 2014). IPS samples were then immediately freeze-dried. Afterwards, these samples were ground and passed through a 100-mesh sieve. All the IPS samples had a moisture content of 6% (w/w, wet basis) after freeze-drying (AOAC, 2005). The products were denoted IPS30, IPS40, IPS50, IPS60 and IPS70 according to the moisture contents in raw materials during the extrusion process.

2.3 Degree of gelatinization (DG)

The degree of gelatinization of native starch and IPS samples was determined by the method of Birch and Priestley (1973) with some modification. 50 mg of samples were added to 50 mL 0.05 M KOH solution. The slurry was then centrifuged for 10 min at 4000 rpm, 1 mL aliquots of the supernatant were added to 1 mL 0.05 M HCl and made up to 10 mL with deionized water. 0.1 mL of iodine reagent (1 g iodine and 4 g KI per 100 mL deionized water) were then added, and after mixing the absorbance was measured at 600 nm against a reagent blank without sample. KOH (0.05 M) and HCl (0.05 M) were replaced by 0.5 M KOH and 0.5 M HCl in the control group. The average of three measurements was taken and the DG was computed using the following equation:

$$DG = \frac{A_1}{A_2} \quad (1)$$

where A_1 is the absorbance of the test group at 600 nm and A_2 is the absorbance of the control group. The determination of DG was based on the formation of a blue iodine complex with released amylose during gelatinization.

2.4 Water absorption and solubility indices

Water absorption index (WAI) and water solubility index (WSI) of native starch and IPS samples were determined by the method of Anderson, Conway, Pfeifer, and Griffin (1969). 2.5 g of ground sample was suspended in 30 mL of distilled water at 30 °C in a 50 mL tared centrifuge tube. The contents were stirred intermittently over 30 min and centrifuged at 3,000 × g for 10 min. The supernatant liquid was poured

carefully into a tared evaporating dish. The remaining precipitate was weighed and WAI was calculated as the weight of precipitate obtained per gram of solid. WSI is the amount of dried solids recovered by evaporating the supernatant from the water absorption test just described as percentage of dry solids. The results were reported as the average of three measurements.

2.5 Pasting properties

A Rapid Viscosity Analyzer (RVA Super 4, Newport Scientific, Australia) was used to determine pasting properties of native starch and IPS samples. 3.0 g of starch samples were mixed with 25.0 mL water and stirred in an RVA container. The rotation speed of the plastic paddle were 960 rpm for the initial 10 s and finally at 160 rpm for the remaining test. These shear rates are according to the standard RVA analysis procedure. The samples were held at 50 ^{o}C for 1 min and heated to 95 ^{o}C at a rate of 6 ^{o}C /min followed by maintaining at 95 ^{o}C for 5 min and cooling to 50 ^{o}C at a rate of 6 ^{o}C /min and finally held at 50 ^{o}C for 2 min. Parameters recorded were peak viscosity (PV, cP), trough viscosity (TV, cP), breakdown viscosity (BD, cP), final viscosity (FV, cP) and setback viscosity (ST, cP). All measurements were repeated three times.

2.6 Polarized optical microscopy

The starch granules of all samples were observed via polarized optical microscopy following the method of Zhang, Zhu, He, Tan, and Kong (2016) with some modifications. 1 mg starch was dispersed in 5 mL pure ethanol (reagent grade) and made up to 50 mL with 50% glycerol. A drop of starch suspension was placed on

the microscope optical contact and covered with a coverslip. The starch granule shape and Maltese cross were viewed under the polarized light microscope (Olympus BX51, Olympus Corporation, Tokyo, Japan) equipped with a CCD camera.

2.7 Scanning electron microscopy

Native starch and IPS samples were stuck onto one side of double-adhesive tape attached to a circular specimen tub. The samples were viewed using an environmental scanning electron microscope (ESEM) (Quanta200F, FEI Deutschland GmbH, Kassel, Germany) at 101 kV and 3.0 spot size. Low vacuum mode was used while operating the ESEM (Liu et al., 2016).

2.8 X-ray diffraction analysis

Wide-angle X-ray scattering measurements of all the lyophilized samples (moisture content around 6%) were using a XRD DI SYSTEM (BEDE Group, UK) with Cu K_α radiation at 40 kV and 30 mA. X-ray diffraction data were collected for 2θ from 4 to 40° at a scanning rate of 0.5°/min at room temperature (Ye et al., 2016).

2.9 Size-exclusion chromatography analysis

The molecular structures of native starch and IPS samples were characterized using SEC as detailed elsewhere (Li, Prakesh, Nicholson, Fitzgerald, & Gilbert, 2016) with minor modifications. Dissolved branched starch molecules were eluted using DMSO solution containing 0.5% (w/v) LiBr as the mobile phase at a flow rate of 0.3 mL/min, and separated using a GRAM pre-column, GRAM 100 and GRAM3000

columns (PSS) in a column oven at 80 °C. SEC separates by the hydrodynamic radius, R_h. The molecular size distribution of branched starch molecules was plotted as the SEC weight distribution, $w_{br}(\log R_h)$. Using the universal calibration assumption and the Mark-Houwink relation, one has for two polymers, a sample and a standard, the relation (see, e.g. Vilaplana & Gilbert (2010a)):

$$K_{standard}\, M^{\alpha(standard)+1} = K_{sample}\, M^{\alpha(sample)+1} \quad (2)$$

Pullulan standards were used for calibration following the Mark-Houwink equation for linear polymers of molecular weight M:

$$V_h = \frac{2}{5}\frac{KM^{1+\alpha}}{N_A} \quad (3)$$

where N_A is Avogadro's constant and $V_h = 4/3\ \pi\ R_h^3$ is the hydrodynamic volume. The Mark-Houwink parameters K and α of pullulan in DMSO/LiBr at 80 °C are 2.424×10^{-4} dL g^{-1} and 0.6, respectively.

Debranched starches were prepared as described elsewhere (Wu, Li, & Gilbert, 2014). These were re-dissolved in DMSO containing 0.5% (w/v) LiBr for SEC analysis, using a GRAM 100, GRAM 1000 as well as a pre-column to obtain the weight chain-length distribution (CLD) of debranched starches. The SEC weight distribution of debranched chains with degree of polymerization (DP) X, $w(\log X)$, obtained from the DRI signal was plotted against X, with X being determined using the Mark-Houwink relationship and M =162.2(X – 1) +18.0 (here 162.2 is the molecular weight of the anhydroglucose monomeric unit and 18.0 is that of the additional water in the end group); K and α for linear starch chains in the eluent of DMSO/LiBr at 80 °C are 1.5×10^{-4} dL g^{-1} and 0.743, respectively. For a linear polymer

(such as debranched starches), the number distribution of chains (obtained by debranching), $N_{de}(X)$, is related to the corresponding SEC weight distribution:

$$w(\log X)=X^2 N_{de}(X) \quad (4)$$

2.10 Statistical analysis

Statistical analysis was carried out using data analysis functions in Origin 8.5 (OriginLab Corporation, Northamptaon, MA). Significant differences between the results were calculated by analysis of variance (ANOVA). Differences at $p < 0.05$ were considered significant.

3. Results and discussion

It is well recognized that starch structure controls starch properties, and that starch molecular structure can be categorized into multiple levels, starting with individual chains (Level 1), the way these chains are joined together (branched structure, Level 2), and high-order structural features such as crystalline and amorphous lamellae. We discuss first the changes in structural features brought about by our IECT process, and then changes in properties, along with explaining the latter in terms of the former.

3.1 Size-exclusion chromatography

SEC weight distributions of starch molecules without debranching (Level 2 structure) of native starch (NS) and IPS samples are shown in Fig. 1, normalized to

the peak maximum of amylose. All starches showed the usual populations of amylose (~ 20 nm) and amylopectin (~ 400 nm) (Fig. 1 and Table 1). The molecules in the range of $R_h \leq 100$ nm are assigned to amylose (Am), and the amylopectin (AP) molecules have a molecular size $100 \leq R_h \leq 4000$ nm. Note that because of shear scission in SEC, the amylopectin SEC distributions in the amylopectin are somewhat degraded from the true values (Cave, Seabrook, Gidley, & Gilbert, 2009), and thus these whole-molecule data cannot be used to quantify amylose content, which is instead obtained from the debranched distributions. The average R_h, found as given by Vilaplana and Gilbert (2010b), of IPS starch molecules were smaller than that of native starch (Table 1). The higher the initial moisture content in IECT treatment, the smaller the starch molecules. The average R_h of IPS70 was 20.7 nm, while that of native starch was 39.2 nm, showing molecular degradation. R_h at the peak maximum of amylopectin decreased from 486 nm for NS to 328 nm for IPS70 (Fig. 1A). At the same time, the ratios of the maximum heights of the amylopectin and amylose components, $h_{Ap/Am}$, also decreased from 1.09 to 0.24. There was no significant difference among the R_h positions of the peaks of amylose molecules of NS and IPS samples (Table 1). This is because these molecules are sufficiently small to be stable against shear degradation under these extrusion conditions (Liu, Halley, & Gilbert, 2010). All above results indicated that the most degradation by IECT treatment occurred on the amylopectin molecules, as expected because of their large size. It is well known that amylopectin is more sensitive to degradation than amylose by extrusion (Della, Vergnes, Colonna, & Patria, 1997).

Typical SEC weight distributions, $w(\log X)$, of debranched starch (Level 1) following hydrolysis by iso-amylase are observed, with a broader peak associated with amylose chains (DP $X \geq 100$) and a bimodal peaks associated with amylopectin chains (DP $X \leq 100$) (Fig. 1B). However, the plot of CLD of debranched rice starch and IPS samples revealed no significant differences. The degradation of the amylopectin molecules by IECT treatment thus did not affect the starch's CLD. Amylose content was defined as the ratio of the area under the curve (AUC) of amylose branches to the AUC of all debranched molecular distribution (including both amylose and amylopectin branches), which also showed no significant differences among the different IPS samples. The above results indicated that the degradation of molecules by IECT treatment mainly occurred in chains between clusters. The α-(1→6) or α-(1→4) glycosidic bonds in the vicinity of the branching points of amylopectin are susceptible to shear degradation during IECT treatment. This phenomenon was similar to previous inferences by Li, Hasjim, Xie, Halley, & Gilbert (2013).

3.2 X-ray diffraction analysis

X-ray diffraction patterns of the native starch and IPS samples are presented in Fig. 2. The native starch exhibited strong peaks at about 15°, 17.2°, 17.9°, and 23° 2θ which are typical A-type X-ray pattern of cereal starches. All peaks were gradually weakened in IPS30 and IPS40, and finally almost disappeared in IPS50-70. These results indicated that most of the crystalline structure of native rice starch were

gradually destroyed by the IECT treatment and became amorphous structures as the initial sample moisture content increased. The crystallinity of native starch was 25.69% and the crystallinities of IPSs were 12.51%, 9.48%, 6.52%, 4.37%, 4.42% respectively (Table 1). The crystallinity result was attributed to the DG (see below) of IPS samples: the higher the water content, the higher DG, therefore the lower crystallinity.

The clear crystallinity peak at 20° in the IPS samples was not found in NS. Ye et al. (2016) and Zhang et al. (2014) also found the absence of a peak at 20^{o} in NS. The crystallinity peak indicates the formation of V-type crystallinity in IPS samples, which could be due to amylose-lipid complexes formed during the extrusion of cereal starch. This could hinder the amylose rearrangements (retrogradation), as previously reported (Wu, Chen, Li, & Wang, 2010), and would reduce the ST in RVA analysis (Table 2), which suggested that IPS samples prepared by IECT had slower short-term retrogradation.

3.3 Scanning electron microscopy and polarized optical microscopy

The morphologies of native starch and IPS samples examined by SEM with 1200× magnification and polarized optical microscope with 1000× magnification are shown in Fig. 3. Native starch granules showed polyhedral shape, with the size range 3–8μm (Fig. 3A), which is a typical morphological structure of rice starch, and is similar to previous research (Fu, Luo, BeMiller, Liu, & Liu, 2015; Zhang et al., 2014). The structure of starch granules was significantly changed after IECT, and hole-shape

structures were found in the IPS samples (Fig. 3B-F). The structure of IPS30 and IPS40 were irregular (Fig. 3B-C) with a few pores. The IPS30 and IPS40 samples are continuous materials formed by gelatinized starch, but there remain small granules, indicated by arrows. The form of the granules are also apparent through the polarized microscopy (Fig. 3b and c). IPS samples gelatinized under 50%-70% moisture content showed continuous and porous aggregates with a honeycomb-like structure, similar to what was reported by Zhang et al. (2014). The gelatinization during IECT treatment involves the absorption of water into granules at elevated temperature, followed by granule swelling and eventual disintegration to form a homogeneous gel. The crystallinity of starch was destroyed and the structure changed into a laminar and porous shaped sponge, resulting in the increased WAI and cold water-swelling capacity.

As shown in Fig. 3a, native rice starch granules showed characteristic birefringence with clear Maltese crosses centered at the hilum under polarized optical microscope, as seen by Deng et al. (2014). There were some granules observed in IPS30 and IPS40 samples (Fig. 3b and c). Most granules aggregated and retained angular and polyhedral shape in IPS30 and lost most angular and polyhedral shape in IPS40, indicating that starch granules under the current IECT conditions of 30% and 40% water content have not been completely disrupted. However, no birefringence can be detected in IPS50, IPS60 and IPS70 granules (Fig. 5d-f), suggesting that the starch was completely gelatinized and the ordered structure completely disrupted. The result from polarized light microscopy observations was consistent with the X-ray

result, showing the change from crystalline to amorphous structure.

3.4 DG analysis

The DG of NS and IPS samples prepared with different moisture content are presented in Table 2. DG of NS was 9.37%, and the DG of all IPS samples were significantly ($p < 0.05$) increased to > 60%. The starch almost gelatinized at 70% moisture content after IECT. When the moisture content was higher in the starting material, the starch granules absorbed water more easily and swelled more quickly and thus gelatinized more easily, resulting in DG increasing with the water content in the raw material.

Gomez and Aguilera (1984) reported the DG of extruded corn starch were from 16% to 63% at the moisture content from 32% to 14%, which showed the DG decreased with increased moisture content. However the DG of starch increased with the water content in the raw material in IECT. The different result may be because the screw speed was too fast (750 rpm) in their work, resulting in shorter residence time. The water would play a role as plasticizer even at a low level of moisture content (below 30%) which would reduce the effect of mechanical shearing and heating during extrusion. The screw speed of IECT was only 37.5 rpm, resulting in a longer residence time, whereby the water would promote the starch gelatinization.

3.5 WAI and WSI analysis

The water solubility and absorption index of native starch and IPS samples

prepared with different moisture contents are given in Fig. 4. Native rice starch was negligibly soluble at room temperature, with WSI was only 0.003%. IECT treatment increased the WSI of indica rice starch significantly ($p < 0.05$). As the moisture content of raw material increased, the WSI of treated rice starches increased to 1.28%, 1.56%, 1.83%, 3.18%, and 4.62% for samples IPS30, IPS40, IPS50, IPS60 and IPS70 respectively.

It has been reported that crystalline structure will affect the WSI of starch (Crochet, Beauxis-Lagrave, Noel, Parker, & Ring, 2005; Ding, Ainsworth, Tucker, & Marson, 2005). In this study, the crystalline structure was disrupted and starch gelatinized, so that the amylose leached out to cause the increase in the WSI of IPS. The degraded starch molecules also were responsible for the increase of WSI of IPS. The WSI were consistent with the average R_h, indicating that the larger the extent small molecules were degraded in the starch, the higher was WSI.

The WAI of native starch was 1.36 and the WAI of IPS30, IPS40, IPS50, IPS60 and IPS70 significantly ($p < 0.05$) increased to 2.46, 2.57, 2.84, 2.92 and 4.12 respectively. The WAI was similar to the research of Yu et al. (2017) who showed the WAI of corn starch was 3.3 to 4.5. WAI is significantly influenced by the magnitude of intra- and inter-molecular interaction within the amorphous and crystalline structure (Fu, Wang, Li, & Adhikari, 2012). When starch was gelatinized by IECT, its crystalline structure was disrupted due to the breaking of inter- and intra- molecular hydrogen bonds, which resulted in more exposed hydroxyl groups for forming hydrogen bonds with water. On the other hand, water molecules could diffuse into the

more amorphous degraded granules more easily than in native starch, and hence the WAI values were higher, as seen by Lee, Kumar, Rozman, and Azemi (2005).

Fig. 5 shows images illustrating the effects of IECT on WSI of starch. The native starch precipitated from the slurry and the supernatant was clear and transparent (Fig.5A). The slurry of IPS30 (Fig. 5B) and IPS40 (Fig. 5C) separated into two layers. The supernatant layers were more turbid and thinner than that of native starch and the precipitate volume was bigger than that in native starch, as a result of the starch granule swelling in water. There was very little supernatant in the IPS50 (Fig. 5D) slurry. The IPS60 and IPS70 slurries almost formed gel (Fig. 5E-F). Fig. 5a-f shows the status of slurry after 30 min without any agitation. Native starch (Fig. 5a), IPS30 (Fig. 5b) and IPS40 (Fig. 5c) showed the same phenomenon as in Fig. 5A-C which were separated into two layers. The IPS60 and IPS70 slurries absorbed water and swelled in cold water (Fig. 5e to f), and therefore, both IPS60 and IPS70 slurries formed more viscous gels than IPS50 (Fig. 5d). There were also some gel at the bottom of IPS30, IPS40 and IPS50 bottles but less so than IPS60 and IPS70.

.

3.6 RVA analysis

Fig. 6 shows the RVA curves of each sample. At low temperature, the viscosities of IPS60 and IPS70 samples increased drastically compared to those of IPS50, IPS40 and IPS30. The viscosity of NS was almost 0 cP at early times. This could be because the IPS samples were partially or almost completely gelatinized by IECT, so that the granules of IPS samples absorbed water more easily and swelled more quickly than

NS at low temperature. The higher water content in raw material, the higher DG, and the more rapid the increase of viscosity at low temperature.

The detailed pasting properties of native starch and IPS samples are shown in Table 2. The peak viscosity, trough viscosity and final viscosity of native starch were 3.36×10^3, 2.34×10^3 and 4.90×10^3 cP respectively, while all viscosities of IPS samples were decreased with the increased moisture content of raw material, and IPS70 showed the lowest peak viscosity (1.98×10^3 cP).

Newport Scientific (1995) reported that the peak viscosity was considered to represent the equilibrium point between swelling and disruption of starch granules. The higher the degree of starch gelatinization in the extruded samples, the less residual granular starch, accompanied by a lower extent of swelling, which led to lower PV in the RVA. The PV result was consistent with the XRD data. Degradation of polymer molecules also reduces their viscosity against shear stress (Buchholz, Zahn, Kenward, Slater, & Barron, 2004). BeMiller (2011) demonstrated that smaller molecules absorb less water and swell less than the bigger molecules, resulting in lower PV in RVA.

BD is calculated from the difference between peak and trough viscosities, as sometimes used to characterize the stability of starch gel (Liu et al., 2016). The BD of native starch was 1.02×10^3 cP, while the BD of IPS30, IPS40, IPS50, IPS60 and IPS70 were all significantly ($p < 0.05$) decreased to 0.90×10^3, 0.90×10^3, 0.89×10^3, 0.78×10^3 and 0.74×10^3 cP, respectively. Since BD reflects the stability of the paste,

this result indicated that the higher the moisture content of the raw material, the higher stability of the paste.

The change of TV was probably because the degraded molecules had smaller size, higher specific surface area, and more open structure, which was likely to facilitate interactions and network formation, resulting in a smaller decrease in viscosity when the temperature was kept at 95^{o}C (Liu et al., 2016). In addition, the molecules of the IPS samples were close to their stable size under extrusion, enhancing heat and shearing stability of the paste after IECT treatment. Liu, Halley and Gilbert (2010) found that larger molecules preferentially cleave to a maximum stable size during extrusion degradation process.

The FV is attributed to reassociation of amylose molecules or short-term retrogradation during cooling. The difference between TV and FV is defined as ST. So we concluded that the decreased ST indicated that IECT could slow the short-term retrogradation of rice starch (Pongsawatmanit, Temsiripong, Ikeda, & Nishinari, 2006). Table 2 shows that the ST of all IPS samples were significantly ($p < 0.05$) decreased compared to that of native starch. The ST of NS was 2.57×10^3 cP, and decreased to 1.44×10^3 cP for IPS70. The decreased ST indicated that IECT could slow the short-term retrogradation of rice starch. The degraded molecule and porous structure led to high water holding capability; the degraded molecule would probably hinder amylose rearrangements and hence retard retrogradation (Satrapai & Suphantharika, 2007). The short chains from degradation are similar to the non-starch

polysaccharides which are responsible for the delay of starch molecule re-association, thereby restraining retrogradation (Liu et al., 2016).

4. Conclusion

This research demonstrated that IPS samples have higher WSI and WAI to cold water, lower ST and BD viscosities during gelatinization, suggesting improved gel stability and retrogradation properties, compared to native starch, heated in RVA, these effects increased with moisture content in the raw material. Rice starch lost integrity and A-type crystalline structure when subjected to IECT, and formed a honeycomb structure after freeze-drying, as observed via SEM. The changes of viscosity and retrogradation properties are related to the degraded molecular size, which mainly occurred in amylopectin. This study thus provides a potential molecular mechanism leading to the corresponding property alternations, and indicates IECT is an effective technique for preparing IPS with desirable properties. Emulsifying activity and rheological behavior are areas for future work.

Acknowledgement

This study was financially supported by the National Natural Science Foundation of China (31571875 and 31271953) and State Key Laboratory of Food Science and Technology, Nanchang University (SKLF-ZZA-201608). We also appreciate the help of Wenwen Yu and Prudence Powell for SEC analysis.

References

Anderson, R., Conway, H., Pfeifer, V., & Griffin, E. (1969). Gelatinization of corn grits by roll-and extrusion-cooking. *Cereal Science Today, 14*(1), 4-7&11-12.

AOAC. (2005). *Official methods of analysis of AOAC International*: AOAC International.

Barron, C., Buleon, A., Colonna, P., & Della, V. G. (2000). Structural modifications of low hydrated pea starch subjected to high thermomechanical processing. *Carbohydrate Polymers, 43*(2), 171-181.

BeMiller, J. N. (2011). Pasting, paste, and gel properties of starch–hydrocolloid combinations. *Carbohydrate Polymers, 86*(2), 386-423.

Buchholz, B. A., Zahn, J. M., Kenward, M., Slater, G. W., & Barron, A. E. (2004). Flow-induced chain scission as a physical route to narrowly distributed, high molar mass polymers. *Polymer, 45*(4), 1223-1234.

Camire, M. E., Camire, A., & Krumhar, K. (1990). Chemical and nutritional changes in foods during extrusion. *Critical Reviews in Food Science and Nutrition, 29*(1), 35-57.

Cave, R. A., Seabrook, S. A., Gidley, M. J., & Gilbert, R. G. (2009). Characterization of starch by size-exclusion chromatography: the limitations imposed by shear scission. *Biomacromolecules, 10*(8), 2245-2253.

Crochet, P., Beauxis-Lagrave, T., Noel, T. R., Parker, R., & Ring, S. G. (2005). Starch crystal solubility and starch granule gelatinisation. *Carbohydrate Research, 340*(1),

107-113.

Deng, Y., Jin, Y., Luo, Y., Zhong, Y., Yue, J., Song, X., & Zhao, Y. (2014). Impact of continuous or cycle high hydrostatic pressure on the ultrastructure and digestibility of rice starch granules. *Journal of Cereal Science, 60*(2), 302-310.

Della, V. G., Vergnes, B., Colonna, P., & Patria, A. (1997). Relations between rheological properties of molten starches and their expansion behaviour in extrusion. *Journal of Food Engineering, 31*(3), 277-295.

Din, Z. U., Xiong, H., & Fei, P. (2015). Physical and Chemical Modification of Starches - A Review. *Critical Reviews in Food Science and Nutrition*, DOI: 10.1080/10408398.10402015.11087379.

Ding, Q., Ainsworth, P., Tucker, G., & Marson, H. (2005). The effect of extrusion conditions on the physicochemical properties and sensory characteristics of rice-based expanded snacks. *Journal of Food Engineering, 66*(3), 283-289.

Fu, Z., Che, L., Li, D., Wang, L., & Adhikari, B. (2016). Effect of partially gelatinized corn starch on the rheological properties of wheat dough. *LWT - Food Science and Technology, 66*, 324-331.

Fu, Z., Luo, S., BeMiller, J. N., Liu, W., & Liu, C. (2015). Influence of high-speed jet on solubility, rheological properties, morphology and crystalline structure of rice starch. *Starch-Stärke, 67*(7-8), 595-603.

Fu, Z., Wang, L., Li, D., & Adhikari, B. (2012). Effects of partial gelatinization on structure and thermal properties of corn starch after spray drying. *Carbohydrate Polymers, 88*(4), 1319-1325.

Gomez, M. H., & Aguilera, J. M. (1984). A physicochemical model for extrusion of corn starch. *Journal of Food Science*, *49*(1), 40-43.

Hedayati, S., Shahidi, F., Koocheki, A., Farahnaky, A., & Majzoobi, M. (2016). Comparing the effects of sucrose and glucose on functional properties of pregelatinized maize starch. *International Journal of Biological Macromolecules, 88*, 499-504.

Hoover, R., Hughes, T., Chung, H. J., & Liu, Q. (2010). Composition, molecular structure, properties, and modification of pulse starches: A review. *Food Research International*, *43*(2), 399-413.

Laovachirasuwan, P., Peerapattana, J., Srijesdaruk, V., Chitropas, P., & Otsuka, M. (2010). The physicochemical properties of a spray dried glutinous rice starch biopolymer. *Colloids and Surfaces B: Biointerfaces, 78*(1), 30-35.

Lee, J. S., Kumar, R. N., Rozman, H. D., & Azemi, B. M. N. (2005). Pasting, swelling and solubility properties of UV initiated starch-graft-poly(AA). *Food Chemistry, 91*(2), 203-211.

Li, H., Prakesh, S., Nicholson, T. H., Fitzgerald, M. A., & Gilbert, R. G. (2016). The importance of amylose and amylopectin fine structure for textural properties of cooked rice grains. *Food Chemistry, 196*, 702-711.

Li, M., Hasjim, J., Xie, F., Halley, P. J., & Gilbert, R. G. (2013). Shear degradation of molecular, crystalline and granular structures of starch during extrusion. *Starch-Stärke, 65*(1), 1-11.

Li, W., Zhang, F., Liu, P., Bai, Y., Gao, L., & Shen, Q. (2011). Effect of high

hydrostatic pressure on physicochemical, thermal and morphological properties of mung bean (*Vigna radiata* L.) starch. *Journal of Food Engineering, 103*(4), 388-393.

Liu, C., Liang, R., Dai, T., Ye, J., Zeng, Z., Luo, S., & Chen, J. (2016). Effect of dynamic high pressure microfluidization modified insoluble dietary fiber on gelatinization and rheology of rice starch. *Food Hydrocolloids, 57*, 55-61.

Liu, C., Zhang, Y., Liu, W., Wan, J., Wang, W., Wu, L., et al. (2011). Preparation, physicochemical and texture properties of texturized rice produce by improved extrusion cooking technology. *Journal of Cereal Science, 54*(3), 473-480.

Liu, W., Halley, P. J., & Gilbert, R. G. (2010). Mechanism of degradation of starch, a highly branched polymer, during extrusion. *Macromolecules, 43*(6), 2855-2864.

Miyazaki, M., Van Hung, P., Maeda, T., & Morita, N. (2006). Recent advances in application of modified starches for breadmaking. *Trends in Food Science & Technology, 17*(11), 591-599.

Newport Scientific (1995). Interpretation. In Newport Scientific (Ed.), *Operation manual for the series 3 Rapid Visco Analyser* (pp. 25–28). Sydney: Newport Scientific Pty. Ltd.

Pongsawatmanit, R., Temsiripong, T., Ikeda, S., & Nishinari, K. (2006). Influence of tamarind seed xyloglucan on rheological properties and thermal stability of tapioca starch. *Journal of Food Engineering, 77*(1), 41-50.

Sánchez, L., Torrado, S., & Lastres, J. (1995). Gelatinized/freeze-dried starch as excipient in sustained release tablets. *International Journal of Pharmaceutics, 115*(2), 201-208.

Sacchetti, G., Pinnavaia, G. G., Guidolin, E., & Rosa, M. D. (2004). Effects of extrusion temperature and feed composition on the functional, physical and sensory properties of chestnut and rice flour-based snack-like products. *Food Research International, 37*(5), 527-534.

Satrapai, S., & Suphantharika, M. (2007). Influence of spent brewer's yeast β-glucan on gelatinization and retrogradation of rice starch. *Carbohydrate Polymers, 67*(4), 500-510.

Vilaplana, F., & Gilbert, R. G. (2010a). Characterization of branched polysaccharides using multiple-detection size separation techniques. *Journal of Separation Science, 33*(22), 3537–3554.

Vilaplana, F., & Gilbert, R. G. (2010b). Two-dimensional size/branch length distributions of a branched polymer. *Macromolecules, 43*(17), 7321-7329.

Wu, A. C., Li, E., & Gilbert, R. G. (2014). Exploring extraction/dissolution procedures for analysis of starch chain-length distributions. *Carbohydrate Polymers, 114*(1), 36-42.

Wu, Y., Chen, Z., Li, X., & Wang, Z. (2010). Retrogradation properties of high amylose rice flour and rice starch by physical modification. *LWT - Food Science and Technology, 43*(3), 492-497.

Ye, J., Hu, X., Zhang, F., Fang, C., Liu, C., & Luo, S. (2016). Freeze-thaw stability of rice starch modified by Improved Extrusion Cooking Technology. *Carbohydrate Polymers, 151*, 113-118.

Yu, C., Liu, J., Tang, X., Shen, X., & Liu, S. (2017). Correlations between the

physical properties and chemical bonds of extruded corn starch enriched with whey protein concentrate. *RSC Advances, 7*(20): 11979-11986.

Zhang, Y., Liu, W., Liu, C., Luo, S., Li, T., Liu, Y., et al. (2014). Retrogradation behaviour of high-amylose rice starch prepared by improved extrusion cooking technology. *Food Chemistry*, *158*, 255-261.

Zhang, Y., Zhu, K., He, S., Tan, L., & Kong, X. (2016). Characterizations of high purity starches isolated from five different jackfruit cultivars. *Food Hydrocolloids*, *52*, 785-794.

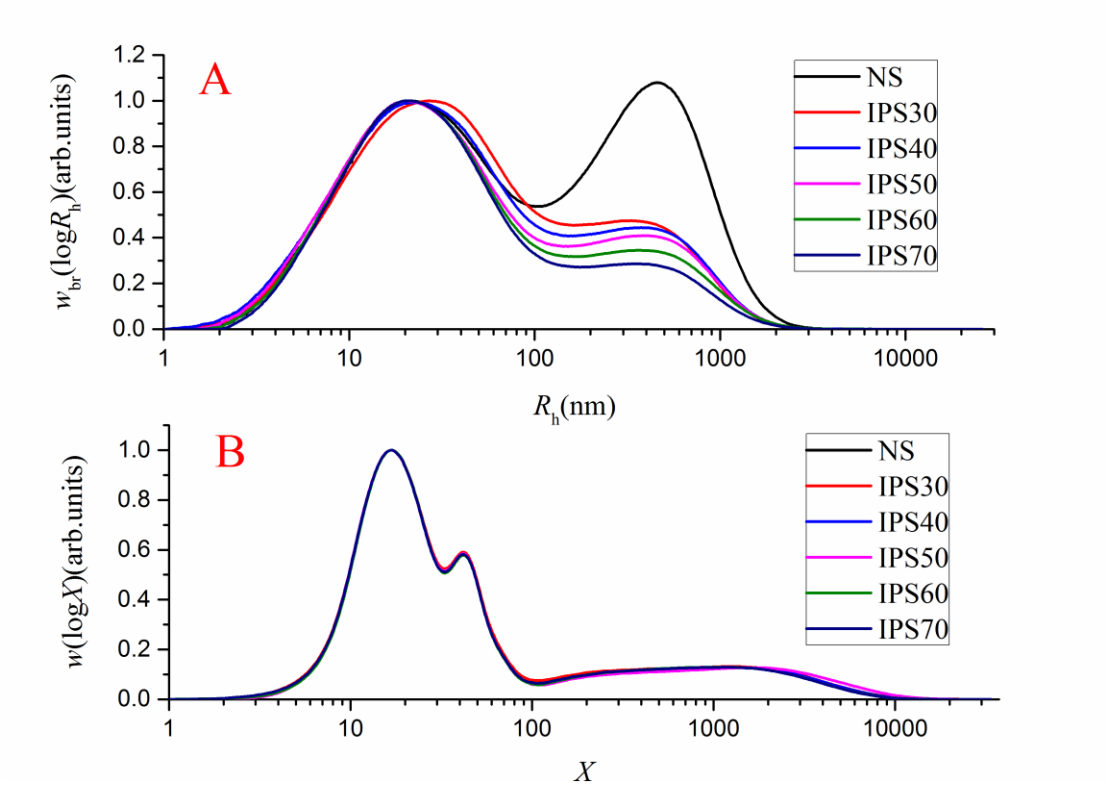

Figure 1. SEC weight distributions of NS and IPS samples. (A) SEC weight distributions of whole starch molecules, $w_{br}(\log R_h)$, normalized to the amylose peak maximum, (B) CLD, $w(\log X)$, of debranched starch molecules, normalized to the height of the first peak.

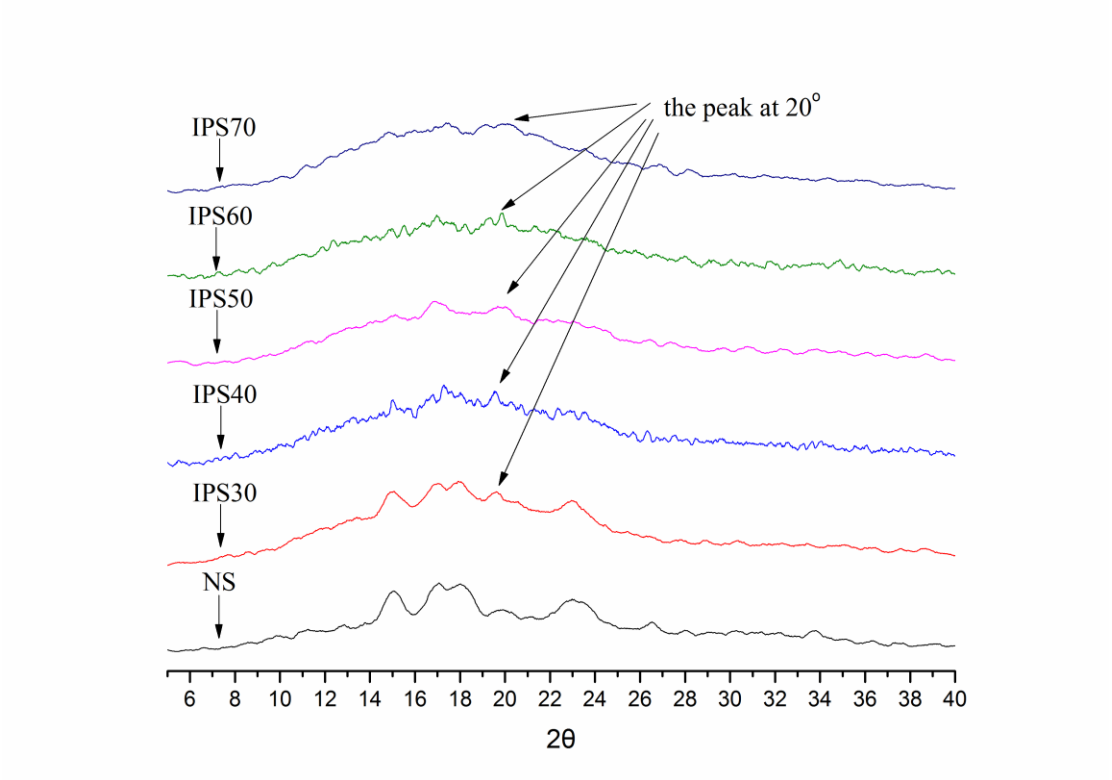

Figure 2. X-ray diffractograms of native starch and IPSs

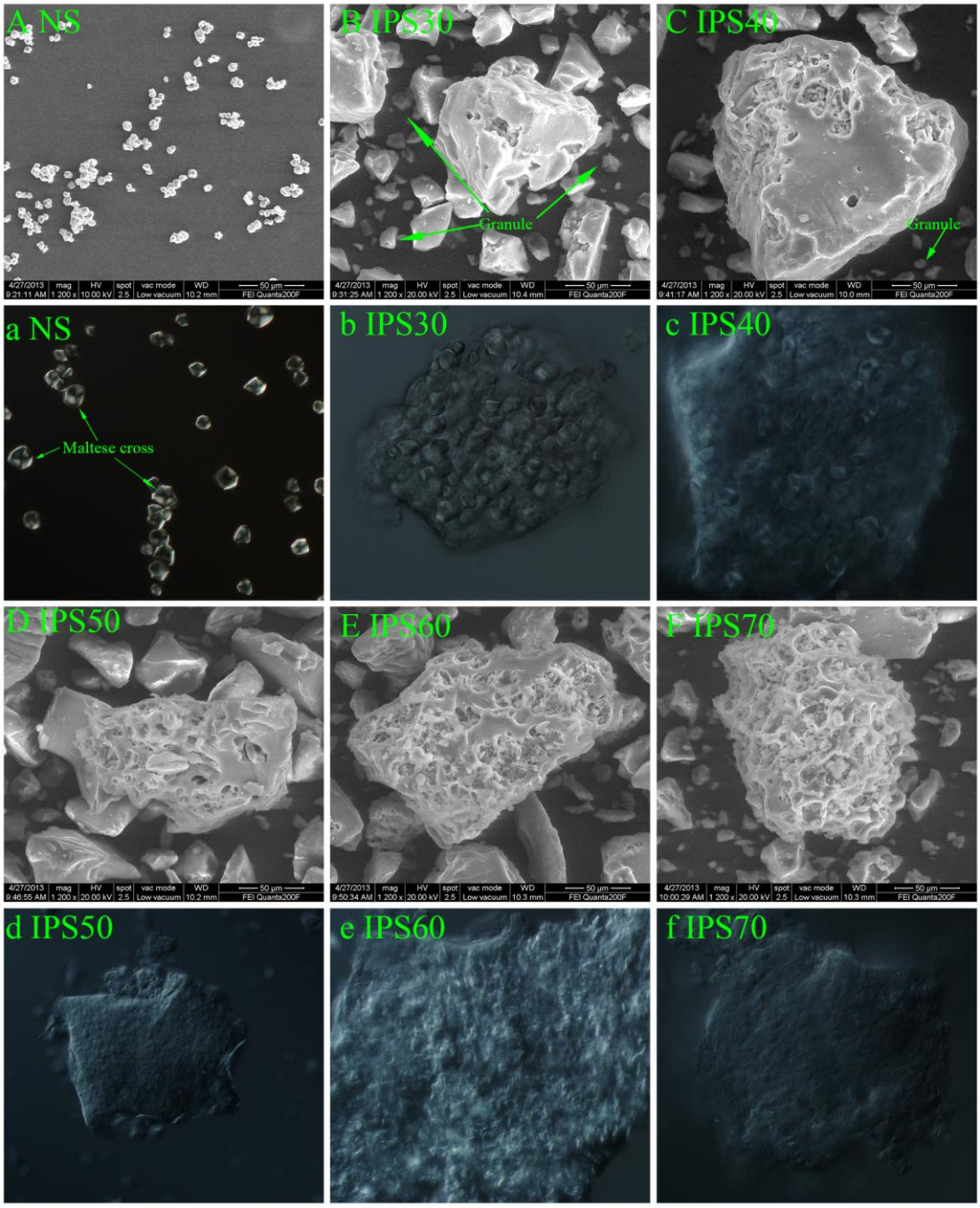

Figure 3. Micrographs of native rice starch and IPS samples under SEM (first row with a scale of 50μm) and polarized light microscope (second row). (A) and (a) NS, (B) and (b) IPS30, (C) and (c) IPS40, (D) and (d) IPS50, (E) and (e) IPS60, (F) and (f) IPS70.

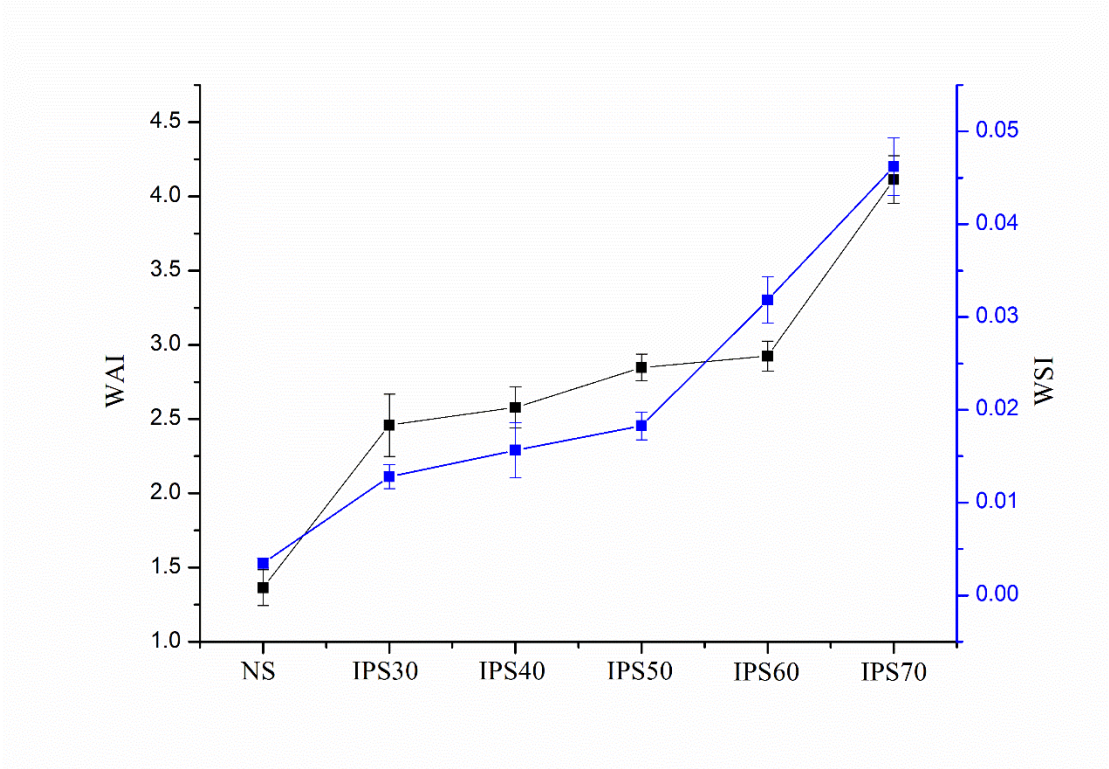

Figure 4. The WAI and WSI at 30 °C of NS and IPS samples prepared by IECT with different moisture content.

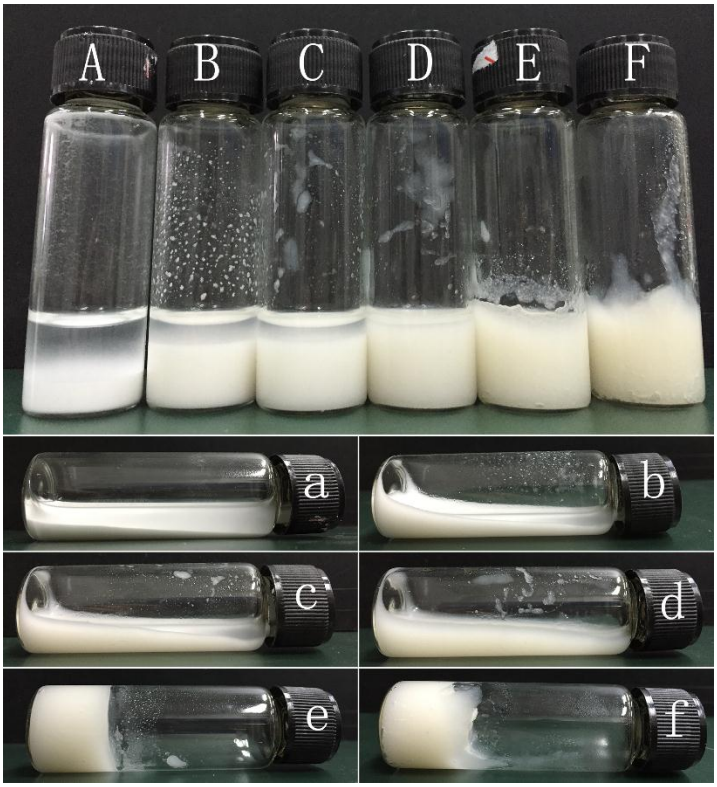

Figure 5. Native starch and IPS samples mixed with distill water at room temperature; (A-F) sample bottle upright. (a-f) sample bottle horizontal: (A/a) NS, (B/b) IPS30, (C/c) IPS40, (D/d) IPS50, (E/e) IPS60, (F/f) IPS70

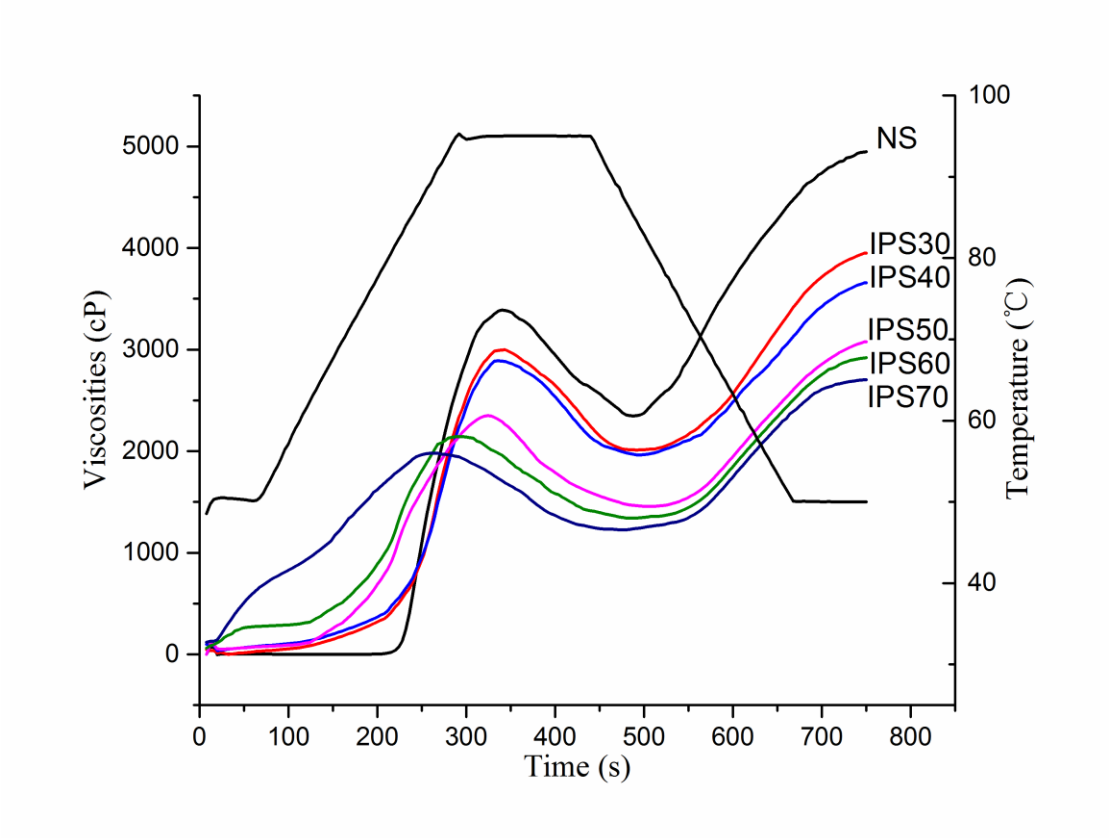

Figure 6. The RVA curves of NS, IPS30, IPS40, IPS50, IPS60 and IPS70.

Table 1

Structural features of Native Starch (NS), IPS30, IPS40, IPS50, IPS60 and IPS70. The quantities $h_{Ap/Am}$, Ap and Am are respectively the ratio of the amylopectin to amylose peak heights, and the R_h of the maxima in amylopectin and amylose.

Sample	Crystallinity (%)	Average R_h (nm)	$h_{Ap/Am}$	Ap (nm)	Am (nm)	Amylose content
NS	25.7±0.8a	39.2±3.2a	1.09±0.00a	486.8±92.0a	20.9±1.3a	0.23±0.00a
IPS30	12.5±0.0b	25.9±2.6b	0.46±0.02b	341.6±57.5c	21.3±0.2a	0.23±0.00a
IPS40	9.5±0.4c	23.7±2.0bc	0.41±0.00c	395.5±27.4bc	20.2±0.6a	0.22±0.01a
IPS50	6.5±0.4d	22.8±1.3bc	0.29±0.00d	393.0±40.7bc	20.6±0.9a	0.22±0.03a
IPS60	4.4±0.7e	21.4±0.6bc	0.29±0.00d	336.1±0.0d	20.2±0.1a	0.22±0.01a
IPS70	4.5±0.4e	20.7±0.5c	0.24±0.01e	328.2±3.7e	19.4±0.1a	0.22±0.00a

[a] Mean ± SD is calculated from duplicate measurements. Values with different letters in the same column are significantly different with $p < 0.05$.

Table 2

Degree of gelatinization and pasting properties of NS, IPS30, IPS40, IPS50, IPS60 and IPS70.

Samples	DG (%)	Peak viscosity ($\times 10^3$cP)	Trough viscosity ($\times 10^3$cP)	Final viscosity ($\times 10^3$cP)	Breakdown ($\times 10^3$cP)	Setback ($\times 10^3$cP)
NS	9.73±0.50 a	3.36±0.02 a	2.34±0.02 a	4.90±0.04 a	1.02±0.02 a	2.57±0.04 a
IPS30	61.4±1.90 b	2.97±0.03 b	2.06±0.00 b	3.92±0.03 b	0.90±0.03 b	1.86±0.02 b
IPS40	71.1±1.48 c	2.88±0.01 c	1.97±0.02 c	3.63±0.04 c	0.90±0.03 b	1.66±0.03 c
IPS50	90.4±0.65 d	2.35±0.00 d	1.46±0.03 d	3.00±0.04 d	0.89±0.02 b	1.53±0.01 d
IPS60	96.8±1.11 e	2.14±0.01 e	1.36±0.02 e	2.89±0.03 e	0.78±0.03 c	1.52±0.03 d
IPS70	97.3±0.31 e	1.98±0.01 f	1.24±0.01 f	2.67±0.03 f	0.74±0.01 d	1.44±0.03 e

[a] Values are mean ± standard deviation (n = 3). Values in the same column followed by different lowercase letters differ significantly ($p < 0.05$).